Research Article | Vol. 30, No. 16 / 1 Aug 2022 / Optics Express 28401
Optics EXPRESS

Pulse temporal scaling of LIDT for anti-reflective coatings deposited on lithium triborate crystals

ERIKAS ATKOČAITIS,* LINAS SMALAKYS, AND ANDRIUS MELNINKAITIS

Vilnius University, Faculty of Physics, Laser Research Center, Saulėtekio Ave. 10, Vilnius 10223, Lithuania
erikas.atkocaitis@ff.vu.lt

Abstract: Anti-reflective (AR) coatings minimize photon losses of optics when it comes to the transmission of light, thus, are broadly used for imaging and laser applications. However, the maximum output power in high-power lasers is limited by the so-called laser-induced damage threshold (LIDT) parameter of optical elements. Often AR coated nonlinear crystals are responsible for such limitations, however, LIDT data is rather scarce. Thus, only limited understanding about LIDT pulse temporal scaling laws for AR coatings exists, which also lacks the specificity about fatigue effect of distinct failure modes. To expand the present knowledge four identical lithium triborate (LBO) crystals were prepared. Each crystal had one side coated with the AR@1064+532 nm coating and the opposite side coated with the AR@355 nm coating. Multiple LIDT tests were then conducted following 1-on-1 and S-on-1 testing protocols at UV and IR wavelengths while varying laser pulse duration. Empirical scaling laws are then investigated for different failure modes and later interpreted using a numerical model.

1. Introduction

The popularity of chirped pulse amplification (CPA) technique is ever-growing as it allows reaching extremely high laser field intensity due to short pulse duration. State-of-the-art systems such as ELI [1] or PETAL [2] therefore require high-quality optical elements, including non-linear crystals for sum and difference frequency generation. However, even the best optical elements have their safety limitations, namely, laser-induced damage threshold (LIDT), usually expressed in units of fluence (J/cm^2, pulse energy per effective area) as well as a useful lifetime (time or dose of irradiation applied until the damage is reached). Coatings, despite their useful optical properties, introduce a new degree of complexity when it comes to the resistance to intense light. The LIDT of a certain optical element depends on various irradiation parameters such as wavelength, beam diameter, time and history of exposure, pulse repetition rate, and pulse duration as well as material properties and its synthesis method. So each parameter may have a different effect on the damage threshold or lifetime of optics. Laser pulse duration (τ) is known to be one of the most important parameters affecting laser damage performance. Various studies [3–19] were conducted on glasses and reported the LIDT dependence on pulse duration. According to the present knowledge, nonlinear excitation, ionization, and fatigue processes govern the damage threshold of optics in a pulsed regime. Stuart *et al.* [3] investigated LIDT scaling laws of fused silica substrates, multi-layer dielectric and metallic gold coatings at IR (λ = 1053 nm) and VIS (λ = 526 nm) wavelengths within 140 fs - 1 ns pulse durations. It was experimentally shown that catastrophic S(=600)-on-1 LIDT of dielectrics scales with pulse duration as $\sim \tau^{0.5}$ for entire ps - ns pulse duration range, while for shorter pulses this scaling law deviates. LIDT scaling was further investigated in femtosecond regime by Lenzner *et al.* [4] and by Mero *et al.* [5] for dielectrics and single-layer coatings. Experiments carried out with $\lambda \sim 800$ nm wavelength indicated $\sim \tau^{0.3}$ dependence below ~20 ps as well as direct correlation with band-gap.

#459391 https://doi.org/10.1364/OE.459391
Journal © 2022 Received 29 Mar 2022; revised 21 May 2022; accepted 22 May 2022; published 19 Jul 2022

Optics EXPRESS

Multiple other studies seem to reproduce $\tau^{0.3}$ - $\tau^{0.5}$ scaling laws [9–19]. For pulses longer than a few μs (continuous wave - CW) LIDT is no longer governed by the electronic processes but rather thermal heating and melting as it was shown by Bliss [6] and Wood [7]. Thus, a thermal balance between deposited and dissipated power defines the damage threshold of the optical element. In the CW regime, it is more convenient to use irradiance as a threshold unit (W/cm^2 - average power per effective area) as it remains constant while changing pulse duration. Constant threshold irradiance scales linearly with pulse duration when converted to units of fluence. It is also known that both thermal damage (CW) and electronic damage (pulsed) in transparent media are also affected by laser beam diameter. Interestingly enough, the bulk damage threshold of silicate glass also features a constant irradiance threshold (similar to CW) even for ultrashort (fs - ns) pulses, when self-focusing of light is suppressed, as reported by Efimov and Juodkazis [8].

When discussing the LIDT scaling of nonlinear crystals there are several important studies to mention. For example, bulk damage threshold of uncoated KDP crystal was found to scale with $\sim \tau^{0.3}$ for 250 ps - 16 ns pulses at IR [20,21] and UV [22] wavelengths. Furukawa *et al.* performed single shot LIDT measurements in LBO bulk material [15] at 1064 nm, 532 nm, and 355 nm wavelengths. They reported $\sim \tau^{0.45}$ LIDT dependence on pulse duration and noticed that shorter wavelength also results in lower LIDT. All above-mentioned studies, however, were limited by relatively short exposure time (either single pulse or a few hundred laser pulses per test site). Prolonged exposure is expected in actual laser systems where other phenomena come into play such as fatigue effect [23], which is responsible for a limited lifetime of optics below the single shot damage threshold. As reported by Möller [24], 192 hours (P = 1.6 W) of third-harmonic generation (THG) resulted in deterioration of LBO crystal performance. Another study [25] reported similar lifetime (P_{IR} = 97 W, P_{UV} = 20.2 W) during THG: damage was initiated after 130 hours with no significant power loss, however, further exposure resulted in 15 % power losses after 371 hours. From lifetime studies one can conclude that fatigue driven damage is either multi-step process or distinct mechanisms of failure co-exist simultaneously.

The existence of distinct failure modes is also indicated by specific damage morphology. It was shown [26–28] that multi-pulse irradiation results either in craters (catastrophic damage) or gentle modifications (laser-induced color changes) of coating that can be resolved using differential interference contrast (DIC) Nomarski microscopy. Color change related failure mode is observed at lower fluence or sooner than catastrophic damage. Unlike catastrophic damage, the nature of color mode is still quite unclear, however, some studies mention possible mechanisms - generation of color centers via multi-photon ionization cause changes of refraction, absorption and refraction [26–28].

Ollé *et al.* [29] reported on the implications that metrology has on the accuracy of temporal scaling laws of LIDT for dielectric materials. However, to our best knowledge, there are no systematic study of LIDTs for AR coated crystals that would consider both fatigue and failure mode analysis for fs - ns pulse length range as well as different testing protocols on the same samples. Furthermore, LIDT scaling in UV spectral range is even less investigated. Accordingly, the purpose of this work is to expand the present knowledge by conducting a case study of LIDT scaling on two types of AR coatings on LBO crystals. This study is conducted at IR and UV wavelengths within 50 fs - 9 ns pulse length region, considering 1-on-1 and S-on-1 testing protocols and failure mode analysis.

2. Materials and methods

This study is organized as follows. First of all, experimental samples are manufactured and irradiated by various laser sources. Next, damage morphology and pertinent LIDT scaling laws are investigated. Finally, theoretical considerations are implemented to discuss experimental results.

Optics EXPRESS

2.1. Preparation of samples

As the study required sufficient area to collect damage statistics, four LBO crystals (12 mm x 12 mm x 10 mm, $\theta = 42.2°$, $\varphi = 90°$ oriented to generate the third harmonic of 1064 nm, angle of incidence is 0°) were prepared. To avoid randomness among samples, all of them were polished within the same batch and later both sides were AR coated simultaneously using ion beam sputtering (IBS) deposition technique. The entrance surface (S_1) was deposited with AR coating for 1064 nm + 532 nm wavelengths using zirconia and exit surface (S_2) was deposited with AR 355 nm using alumina as a high-index material. Silica was used as low-index material in both cases:

- S_1: AR <0.2%, 1064 nm + 532 nm (n_L - SiO_2, n_H - ZrO_2);
- S_2: AR <0.2%, 355 nm (n_L - SiO_2, n_H - Al_2O_3).

2.2. Experimental setup

The samples were measured on front surface of each coating (S_1 with IR (1064nm, 1030 nm) wavelengths and S_2 with UV (355 nm, 343 nm) wavelengths) according to 1-on-1 and S-on-1 testing protocols [30]. The discrimination between LBO and AR coating damage was ensured by locating the focused beam exactly on the front surface of the coating before every measurement. At damaging fluence only the coating is being affected, however, with further increase of fluence filamentation effects within LBO bulk damage due to self-focusing was noticed as well. However, in this study fluences were operated below those fluence values. For every pulse duration measurements were conducted for fixed pulse classes, namely 1 pulse per site, 10, 100, 1000, 10000, and 10^5 pulses per test site. The distance between the sites was equal to three beam diameters ~100 μm. In 50 fs - 10 ps pulse duration range each test was conducted using a matrix of 250 test sites as the damage threshold was rather deterministic. Fluence ramping among levels was not larger than 16% from the previous fluence value for all pulse durations. Accordingly, LIDT was estimated as an average of lowest damaging fluence and highest-non-damaged below. For pulse duration of 100 ps and longer damage process became non-deterministic, thus amount of test sites in measurement matrix was extended to 600 to improve the statistical reproducibility of the LIDT estimate. In this case LIDT was estimated by using classical approach: damage probability curve was fitted to extract highest fluence level featuring 0% probability of damage. Experiments were conducted in 50 fs - 9 ns pulse length range at IR (1030 nm and 1064 nm) and UV (343 nm and 355 nm) wavelengths with the fixed laser repetition rate of 1 kHz while maintaining 29 - 35 μm beam diameter at $1/e^2$ level. All pulse durations were carefully measured using two techniques. For shortest pulse durations commercial auto-correlator (50 fs – 10 ps) was used, while for 150 ps and 9 ns pulses it was measured directly with fast photo-detector and oscilloscope: both having broad enough spectral bandwidth, not limiting pulse duration. The principal scheme of the experimental setup is shown in Fig. 1. To access different pulse durations three different lasers were used: for 50 fs measurement - Legend (Coherent) in combination with HE Topas OPO system (Light Conversion) with onset wavelength of 1064 nm and third harmonic of it, for 200 fs - 10 ps measurement - Pharos (Light Conversion) with fundamental wavelength of 1030 nm and third harmonic of it, generated by separate non-linear crystals, and for 10 ps - 9 ns measurement - Atlantic 80 (Ekspla). At 10 ps pulse duration Atlantic 80 has built-in 3rd harmonic module with fundamental wavelength of 1064 nm, while for longer pulse durations third harmonic was generated with separate non-linear crystals. In 3rd harmonic case appropriate optics were used in order to filter fundamental and 2nd harmonic wavelengths. Before and after exposure all samples were visually inspected by Nomarski microscopy to identify distinct failure modes and their thresholds.

Optics EXPRESS

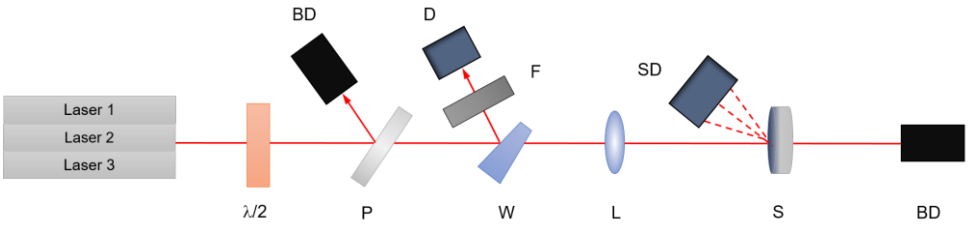

Fig. 1. Experimental setup: Laser 1 - Pharos (Light Conversion), Laser 2 - Atlantic 80 (Ekspla), Laser 3 - Legend (Coherent) + HE TOPAS OPO (Light Conversion), $\lambda/2$ - wave plate, P - polarizer, BD – beam dump, W – wedge, F – filters, L – lens, D – energy diode, S – sample, SD – scattering diode.

2.3. Analysis method

There are many phenomena involved (such as electronic photo-absorption and subsequent lattice heating) in the process of laser-induced damage. In most cases of pulsed regime the primary cause of damage is electronic excitation (either localized – via defect-states or not – in host matrix), however, in non-deterministic damage at ns pulse durations LIDT could be overestimated due to low defect density for catastrophic damage mode.

To interpret experimentally obtained LIDT results consider a model of dielectric material consisting of valence (VB) and conduction (CB) bands populated by electrons. When an electric field is applied, photoionization starts taking place and it is transporting VB electrons to the CB. Further, free electrons in CB are heated by inverse bremsstrahlung in laser field up to the critical kinetic energy so that impact ionization is initiated. As the process continues impact ionization is leading towards the avalanche process. The simplest model that describes such electron generation process is the so-called single-rate equation (SRE) suggested by Stuart *et al.* [3]:

$$\frac{d\rho}{dt} = w_{\mathrm{MPI}}\rho + \alpha I\rho - \gamma_{\mathrm{R}}\rho, \tag{1}$$

where ρ is generated free electron density in CB. The first term on the right-hand side of the Eq. (1) is responsible for electron generation rate from VB to CB defined by Keldysh multi-photon ionization (MPI) rate [31], α is avalanche ionization (AI) constant, I is laser intensity and γ_{R} is electron recombination rate (RE). Although this model is oversimplified, it is intuitive and helps to understand the major trends of phenomena, which will help to discuss experimental results. In Fig. 2 the role of each factor in SRE on LIDT scaling law is briefly exemplified by considering a simplified fictitious dielectric material. To generate this graph a multi-photon process (6 photons) is assumed with avalanche and recombination. Critical free electron density corresponding to plasma frequency ($\sim 10^{21}$ cm^{-3}) was used as a damage criterion.

Firstly, in the inset, the effect of band-gap (or wavelength) on the LIDT scaling law is investigated when only MPI is involved. As can be seen, the MPI process alone, when the condition is 6-photon process, resulted in the LIDT scaling of $\sim \tau^{0.87}$. When wavelength or band-gap is changed MPI contribution is affected: in the case of two-photon process LIDT scaling law transforms to $\sim \tau^{0.5}$. When the avalanche ionization process (solid red and black curves) is involved, LIDT curves become less sensitive to pulse duration at longer pulse durations. Finally, the effect of carrier recombination is non-negligible (dash-dot curves): RE bends the LIDT curves upwards for pulse duration that is longer than onset recombination time. A case where only MPI and RE are involved (dotted curves) is also considered: notably, the recombination process makes the LIDT curves steeper, thus, slightly increasing the exponent of the MPI scaling law. The exemplified scenarios suggest that LIDT scaling is not universal but rather dependent on material and irradiation conditions. For example, pulse duration exponent of 0.5 or higher

Optics EXPRESS

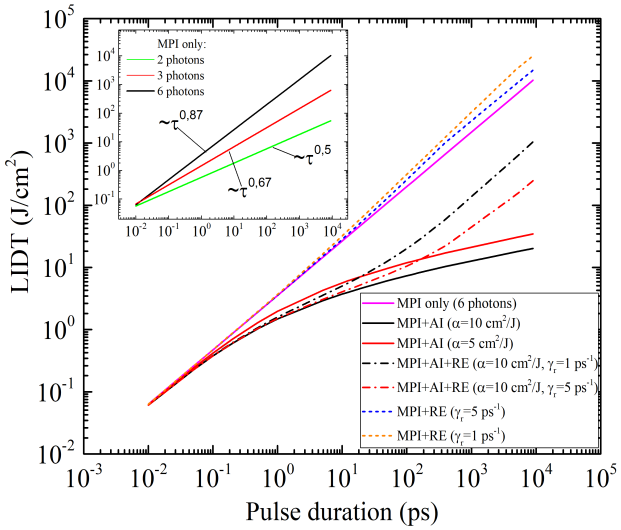

Fig. 2. Effect of individual parameters of SRE model on LIDT scaling law.

indicates MPI and recombination dominated process while lower than 0.5 exponent suggests that damage mechanism is strongly affected by avalanche ionization. The model also suggests that different scenarios are possible when pulse duration or wavelength is changed.

Although the simplicity of the SRE model reveals the main trends of the electronic excitation process, the model itself has limitations: carrier energy in CB is not considered which does not describe the full picture. Kaiser [32] and then Rethfeld [33] suggested a multi-rate equation (MRE) approach which takes into account not only electron density in CB but also their kinetic energy within CB. After reaching critical energy, excited electrons collide with surrounding VB carriers causing AI process by losing kinetic energy and relaxing to the bottom of CB. This model seems to give more consistent results when analyzing experimental data. To simplify the complexity of MRE model a delayed-rate equation (DRE) approach was recently proposed by Déziel *et al.* [14]. The simplicity of DRE in comparison to MRE lies within the ability to track the mean kinetic energy of the electrons and holes with one equation instead of multiple equations for every electron level:

$$\frac{d\rho}{dt} = w_{\mathrm{MPI}}\rho_{\mathrm{n}} + \sum_{s=e,h} \gamma_{\mathrm{n}}^{\mathrm{s}}\zeta^{\mathrm{s}}\rho - \gamma_{\mathrm{R}}\rho. \tag{2}$$

Here electron generation is weighted by the density of neutral atoms $\rho_{\mathrm{n}} = \rho_{\mathrm{mol}} - \rho$, where ρ_{mol} is molecular density of the material. Fraction of carriers (holes and electrons) that have an energy higher than critical is calculated by

$$\zeta^{\mathrm{s}} = \mathrm{erfc}(r_{\mathrm{s}}) + \frac{2r_{\mathrm{s}}}{\sqrt{\pi}}\exp(-r_{\mathrm{s}}^2), \tag{3}$$

where $s = (e, h)$ and

$$r_{\mathrm{s}} = \sqrt{\frac{3E_{\mathrm{c}}}{2E_{\mathrm{k}}^{\mathrm{s}}}}. \tag{4}$$

Here E_{c} is critical energy of electron that is required to trigger impact ionization event and $E_{\mathrm{k}}^{\mathrm{s}}$ is gained mean kinetic energy of the carriers. Further in the study the DRE model is used while interpreting experimental results.

Optics EXPRESS

3. Results and discussion

The section is organized as follows: firstly, damage morphology after single-shot and multi-shot irradiation is analyzed, then LIDT scaling laws are empirically derived for distinct failure modes and protocol of irradiation and finally, possible mechanisms of damage using the rate equation model are discussed.

3.1. Damage morphology

First of all, let us briefly overview images of typical damage morphology obtained by DIC microscopy. Two types of damage could be distinguished, namely, catastrophic damage – features ablation craters (causing scattering of light: not shown here) and non-catastrophic damage – a laser-induced modification, barely apparent as color change: always reproduces the shape of the beam and does not cause any light scattering in damage detection. Sorting of damage morphology into different categories allowed us to interpret damage statistics for each failure mode separately as well as analyze pertinent scaling laws individually. In Fig. 3 damage morphology initiated by IR laser pulses is outlined. In the case of short pulses (<10 ps) color change was observed at fluence levels below catastrophic damage for both single- and multi-shot irradiation. Catastrophic damage was initiated in all cases for higher fluence, however, color changes are not apparent for pulse duration >10 ps, thus, indicating the transition of dominating damage mechanism. From analytical simulations it is safe to assume that color changes become apparent in cases when generated free electrons do not reach critical plasma density (it is lower than $\sim 10^{21}$ cm^{-3} and is equal to $\sim 10^{18}$ cm^{-3}) – it is not enough to cause an efficient avalanche. At higher fluences avalanche ionization becomes very efficient and catastrophic damage is reached at critical plasma density ($\sim 10^{21}$ cm^{-3}). Although the seeding electrons are generated in nonlinear way, the difference in laser fluence that generates $\sim 10^{18}$ cm^{-3} and $\sim 10^{21}$ cm^{-3} electrons is negligible (in logarithmic scale) due to efficient avalanche at longer durations than 10 ps.

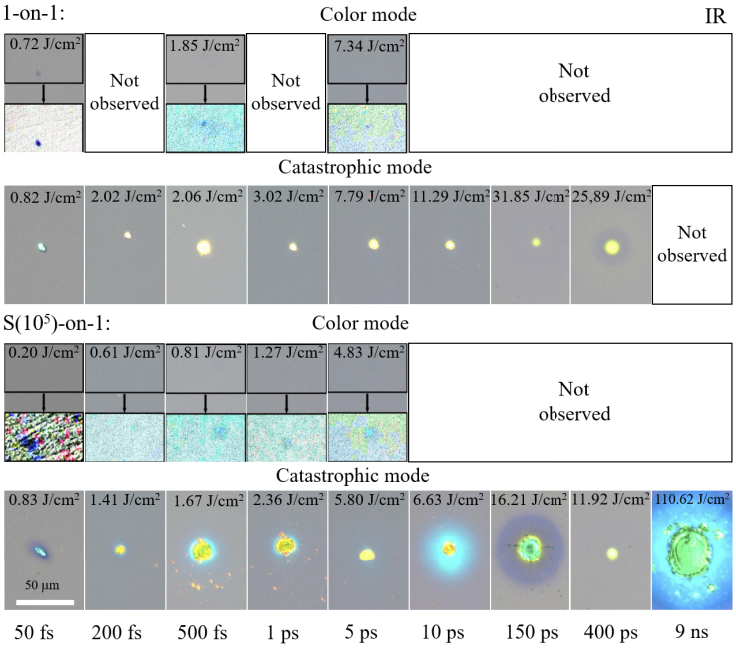

Fig. 3. Damage morphology obtained at threshold fluence values (see Fig. 6(a) and (b)) on S_1 coating at IR wavelengths for all the investigated pulse duration.

Optics EXPRESS

In the case of UV irradiation, similar trends are observed (illustrated in Fig. 4). In all cases laser-induced color changes are better seen for multi-shot irradiation with shorter pulse duration, while single-shot irradiation produces either negligible modifications or abrupt catastrophic damage.

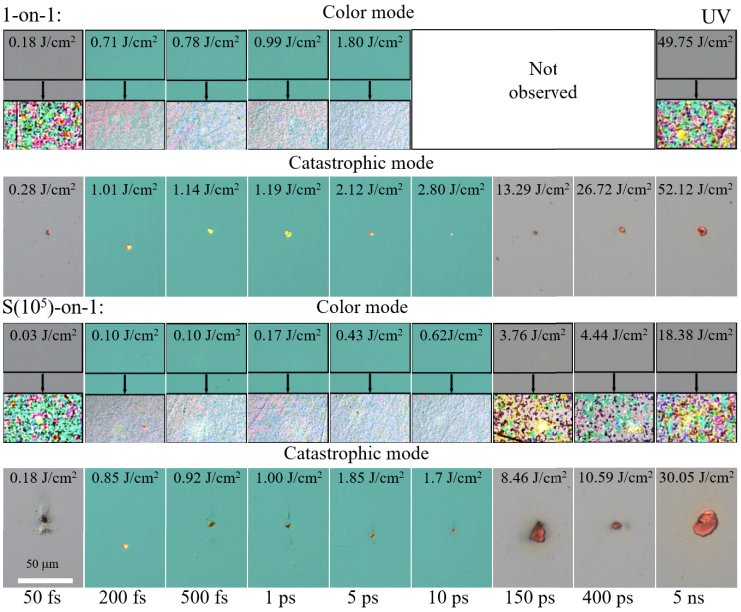

Fig. 4. Damage morphology obtained at threshold fluence values (see Fig. 6(c) and (d)) on S_2 at UV wavelengths for all the investigated pulse durations.

Damage caused by extrinsic defects in the AR coatings and in the Beilby layer of the polished LBO crystal surfaces generally cannot be overlooked, however, in this case rather small beam diameter is used and no pinpoint morphology is observed for color change type damage. Therefore, it is safe to assume that color change is not caused by Beilby layer defects. However, this is most likely the case for catastrophic damage.

3.2. LIDT results

In Fig. 5 normalized (to 1-on-1 value) LIDTs are illustrated as a function of incident number of laser pulses per test site. Each curve was obtained for individual failure mode (either catastrophic damage or color change). First, let us overview color mode results in Fig. 5(a) and 5(b). It can be noticed that both coatings start wearing out almost immediately (after 10 - 100 pulses) and a continuous LIDT drop with an increasing number of pulses at both wavelengths is seen. It is worth mentioning that for color change associated fatigue is wavelength-dependent: at IR 35 - 70 % LIDT drop is observed from its initial value while at UV decline reaches 65 - 90 %. However, the normalized fatigue effect shows weak or no pulse duration dependence when the wavelength is fixed.

In the case of catastrophic damage (Fig. 5(c), 5(d)) different fatigue behavior can be observed: a pulse duration dependence at IR and UV wavelengths - the longer the pulse duration, the stronger the fatigue effect. Here at IR wavelength LIDT drops by a few percent at 50 fs and down to 55 % at 400 ps while in UV instance LIDT drops by 12 - 60 % from its initial value. Secondly, for most cases, fatigue is noticeable only until approximately 1000 pulses at IR, after which it tends to saturate to the so-called fatigue limit, however, there are cases when LIDT declines

Optics EXPRESS

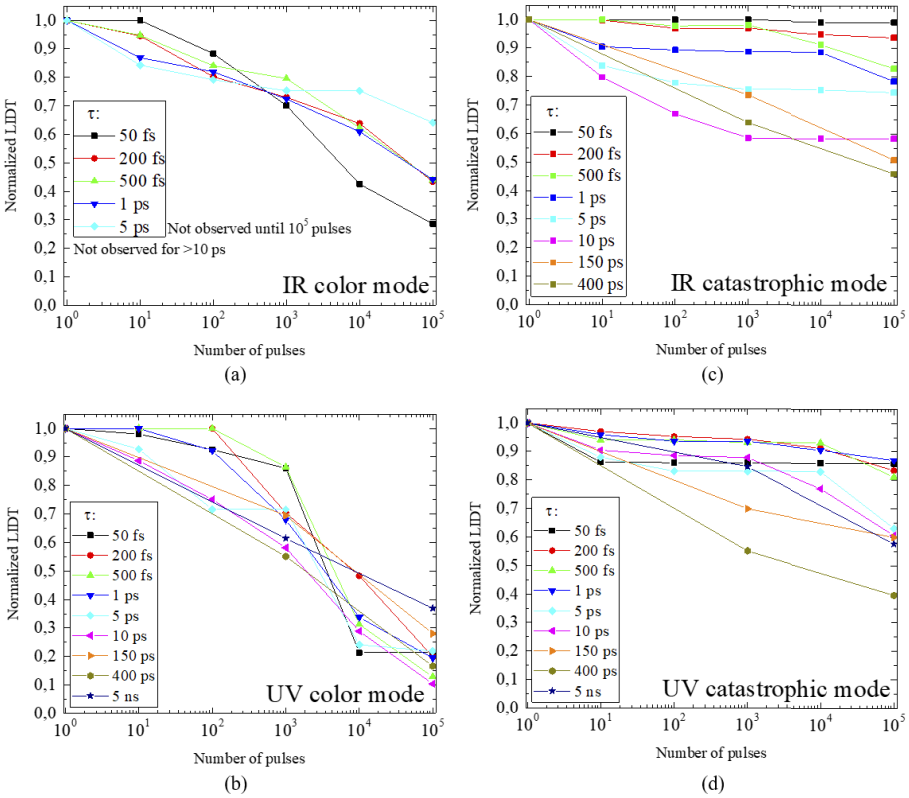

Fig. 5. Fatigue effect of color mode and catastrophic damage: (a) color mode at IR (on S_1), (b) color mode at UV (on S_2), (c) catastrophic damage at IR and (d) catastrophic damage at UV.

further. The observed differences in fatigue behavior between color mode and catastrophic damage suggest differences in initiation mechanisms, as reported by Smalakys *et al.* [27].

As it is seen from the graphs, strongest fatigue is for color mode and shortest pulse durations, thus suggesting that fatigue is directly related to MPI regime and electronic excitation based modification of the material. As this is multi-shot effect, fatigue most likely arises from laser induced atomic level/lattice defects but not macroscopic defects. Macroscopic defects are responsible for catastrophic failure and do not show strong fatigue (at IR wavelength and long pulse duration) [27]. As thermal decay is the same for all pulse durations and much faster than the period between repeating pulses thermal accumulation is not expected to be a primary reason of fatigue [34].

3.3. Empirical scaling laws

Now let us analyze 1-on-1 and S(10^5)-on-1 LIDT results in absolute scale as a function of pulse duration. When experimental LIDT data are plotted on a log-log scale, each failure mode can be represented by a linear trend. Accordingly, data can be approximated by power-law relation $LIDT = a\tau^b$. It is obvious that both failure modes feature distinct scaling and must be analyzed in separation from each other.

LIDT pulse temporal scaling is summarized in Table 1. Exposure at every test site by a single laser pulse produced an almost negligible difference between color change and catastrophic LIDTs for both IR and UV wavelengths (Fig. 6) and only a weak difference in scaling laws. One

Optics EXPRESS

can note that color mode LIDT scales as $\tau^{0.55}$ and catastrophic damage LIDT as $\tau^{0.4}$ in IR case. With the longest IR pulse duration (9 ns) catastrophic damage was not reached with a single laser shot with a maximum available fluence of ~110 J/cm^2, indicating that the intrinsic threshold of the coating is higher or defect density is rather low.

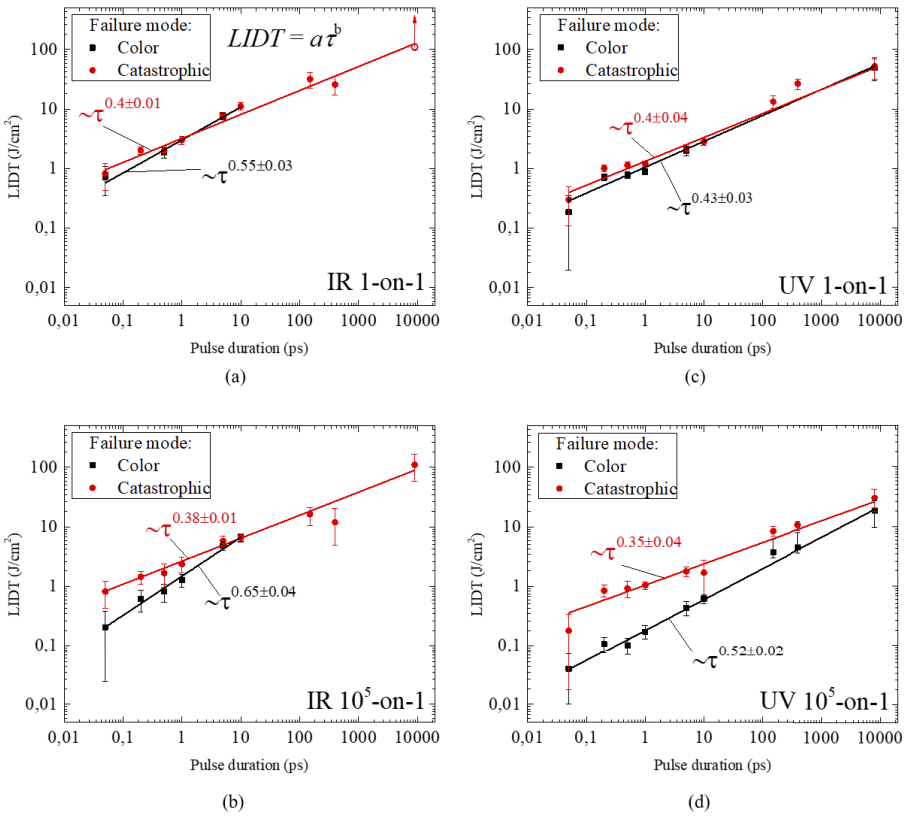

Fig. 6. LIDT scaling laws for damage modes: (a) - 1-on-1, (b) - 10^5-on-1 pulses at IR wavelength on S_1, (c) - 1-on-1 and (d) - 10^5-on-1 pulses at UV wavelength on S_2. Data were approximated with power law curve and respective scaling are shown in the graphs.

Table 1. Summarized LIDT exponents of pulse temporal scaling laws for respective coating material, discussed in Fig. 6.

Coating H material	Color 1-on-1	Catastrophic 1-on-1	Color S-on-1	Catastrophic S-on-1
ZrO_2	0.55±0.03	0.4±0.01	0.65±0.04	0.38±0.01
Al_2O_3	0.43±0.03	0.4±0.04	0.52±0.02	0.35±0.04

In contrast to single-shot exposure, 10^5 pulses produced more obvious differences in LIDT scaling between separate failure modes: IR color mode - $\tau^{0.65}$, while catastrophic damage scaling was similar to the single-shot case - $\tau^{0.38}$. An increasing number of laser pulses also results in a larger difference between color and catastrophic LIDTs which is especially expressive in the femtosecond pulse duration range. The obtained results for catastrophic damage mode scaling are in good agreement with previous studies [15,20,21]. In the case of UV irradiation, a similar trend is seen for 1-on-1 color and catastrophic damage: both have almost the same scaling law - $\tau^{0.43}$ and $\tau^{0.4}$ respectively. Similarly, an increased number of pulses shows clear LIDT separation

Optics EXPRESS

between damage modes. The speciality of multi-shot UV case is that failure modes can be easily separated for the entire 50 fs - 9 ns pulse duration range: here $\tau^{0.52}$ and $\tau^{0.35}$ scaling laws are observed for color mode and catastrophic damage respectively.

With UV wavelength, it is a color mode that has a classic $\sim \tau^{0.5}$ LIDT scaling law while catastrophic damage seems to follow similar scaling of $\tau^{0.35-0.4}$ laws for both IR and UV wavelengths. Catastrophic damage indicates no strong dependence on the number of incident laser pulses. In contrast, LIDT scaling of color mode is rather sensitive to the total number of incident pulses, thus indicating the presence of a cumulative process, most likely driven by nonlinear absorption and formation of color centers. Furthermore color mode is also more sensitive to the wavelength: scaling for different pulse classes at different wavelengths varies - $\tau^{0.55-0.65}$ at IR and $\tau^{0.43-0.52}$ at UV wavelength. These results suggest that either two competing or interrelated damage mechanisms dominate each failure mode, which will be further discussed in the next section. When comparing our experimental data on coated LBO crystals with other studies on dielectric coatings, uncoated glasses and non-linear crystals [3,5,12,20]), no clear transition is observed in scaling law while changing pulse duration from ps to fs at IR wavelength. There is no good explanation for such a result, however, it is obvious that defect-driven (catastrophic) damage is material- and thus defect-density-dependent for longer pulses. In this case, the total sampled area and testing approach become statistically important. Furthermore, color changes are difficult to detect, therefore, might be overlooked or not considered as the initiation of damage. Interestingly, in the case of IR, it can be noted that color changes emerge exactly at the previously reported transition point (20 ps) - shorter pulses produce a color change, while for longer pulses such changes are screened by catastrophic damage.

3.4. Discussion on damage mechanisms

To interpret LIDT data and the physics behind damage mechanisms a delayed-rate equation approach is considered as introduced in Sec. 2.3. As each AR coating is consisting of two types of layers (H and L index), it was chosen to limit analysis for H material only, as it defines LIDT of the whole coating due to lower band-gap [5]. Since two failure modes are specific for every single coating, it is sought to describe response of a material with a single set of material parameters, however, damage criteria pertinent to specific failure mode is assumed to be different. The material parameters used for simulations of H material are given in Table 2 for both coatings. Two criteria - critical electron density, corresponding to wavelength dependent plasma frequency, $\rho \approx 10^{21}$ cm^{-3} and sub-critical electron density $\rho \approx 10^{18}$ cm^{-3} initiating the color changes - were investigated for both UV and IR coatings. The process of obtaining theoretical LIDT curves is as follows: with a given set of material parameters, laser fluence is varied at every pulse duration until particular damage criteria are reached. First of all, sub-critical density (resulting in color change) is reached, and by further increasing the fluence a critical plasma density (leading to catastrophic damage) is reached. The predicted LIDT is directly compared with experimental data within measurement errors. The results of DRE simulation are plotted against two edge cases of experimental data, namely 10^5-on-1 catastrophic damage and color change in Fig. 7.

Table 2. Dielectric material parameters associated with theoretical simulations. Plasma damping γ, energy bandgap E_g, recombination rate γ_r, effective mass of an electron (m_e) and hole (m_h) are set by fitting the data. σ, ρ_{mol} and n are gathered from [14].

	γ (fs^{-1})	γ_r (ps^{-1})	m_e	m_h	E_g (eV)	σ (10^{-25}/m^2)	ρ_{mol} (10^{22}cm^{-3})	n
ZrO_2	1.0	2.0	0.4	0.7	4.0	6.175	1.0	2.2
Al_2O_3	1.0	0.3	0.2	0.2	6.0	13.3	1.0	1.76

Firstly, let us analyze the cases of catastrophic damage. All the processes (MPI + AI + RE) are required to fit catastrophic mode, however, for the sake of clarity MPI-only curves are also

Optics EXPRESS

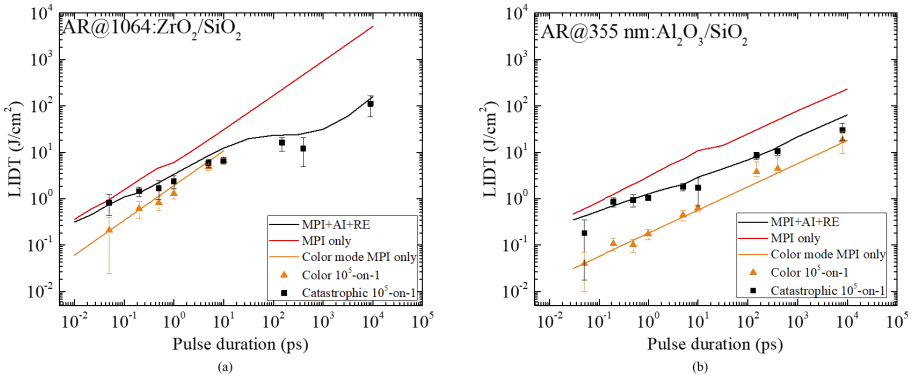

Fig. 7. Experimental data approximated by DRE model [14]: (a) - AR coating for IR wavelength, (b) - AR coating for UV wavelength. In both cases different critical electron density was used: for 1-on-1 catastrophic and color damage - 10^{21} cm^{-3} and for 10^5-on-1 color mode - 3×10^{18} cm^{-3}.

included. The damage process initiated by multi-photon absorption governs LIDT at short pulse duration (<50 fs) which is in good agreement with other studies [4,14,35]. For longer pulses, avalanche ionization and recombination processes become significant and cause noticeable deviation from the MPI-only curve (see Fig. 7(a)) that also features a characteristic transition (both at IR and UV wavelengths) predicted by Keldysh model [14,31,35].

S(10^5)-on-1 color mode data cannot be described using the same damage criterion. Nonetheless, one can observe that MPI-only (red curve) obtained with the same set of parameters goes in parallel to experimentally measured data representing color changes. Since color changes are most likely not caused by critical plasma density, a reduced number of electrons as a damage criterion was explored. By varying electron density to $\rho \approx 10^{18}$ cm^{-3} was reached (see Fig. 7(a) orange curve). It was sufficient to reproduce color change data with the same model and material parameters. Accordingly, the MPI-only process was sufficient to explain such color changes as AI leading to catastrophic damage requires much higher fluence (is not efficient at lower fluence and thus low plasma density). In this case, every laser pulse seems to cause a nonlinear excitation of material leading to gentle cumulative modification, however, only the long-term cumulative process makes such color changes apparent to DIC microscopy. Our preliminary results show that such a process would eventually lead to catastrophic damage, however, this topic deserves a separate study. In the case of IR, color changes are screened by catastrophic damage for pulse durations above (>10 ps).

In the UV case (see Fig. 7(b)), the general trend for S(10^5)-on-1 damage stays the same as IR catastrophic damage since it is mainly due to multi-photon absorption and avalanche ionization in the whole pulse duration range. Carrier recombination does not have a strong effect on LIDT in the nanosecond range. Similarly to IR case, a color mode cannot be explained with critical plasma density as well, therefore, the threshold criteria was lowered to $\rho = 3{\times}10^{18}$ cm^{-3}. What is interesting in this situation is that color mode after 10^5 pulses appears at every measured pulse duration and there is no mode screening - in this instance, it is two-photon ionization. The gap in UV between damage modes seems to be larger than in IR.

4. Conclusions

To sum up, LIDT dependence on pulse duration was investigated on AR-coated LBO crystals by considering failure modes at UV and IR wavelengths. For the first time, laser-induced color changes were analyzed in terms of LIDT pulse temporal scaling. Direct comparison of LIDT data

Optics EXPRESS

with SRE and DRE models suggests that LIDT scaling is not universal, but rather failure mode dependent. Multi-photon ionization dominates the damage process at short pulse duration and also leads to laser-induced color changes at longer pulse duration, this is especially highlighted with prolonged multi-pulse exposure. Accordingly, MPI dominated color changes are directly dependent on the band-gap of the material as well as wavelength. Experimentally investigated LIDTs of color changes induced with 1 to 10^5 pulses feature $\tau^{0.55-0.65}$ at IR and $\tau^{0.43-0.52}$ scaling at UV wavelength. SRE simulations predict that the exponent of 0.5 is associated with a two-photon process while the larger exponent might be attributed to the absorption process with more photons involved. Simulation results also suggest that both failure modes can be reproduced by using the single material model with the same parameters, however, damage criteria (namely, sub-critical and critical electron density) must be different for a particular failure mode. It was also noticed that LIDT scaling related to catastrophic damage behaves similarly for both wavelengths and scales as $\tau^{0.35-0.4}$ within the entire range of investigation (50 fs - 9 ns) for 1-on-1 and 10^5-on-1 exposure. The exponent of τ with less than 0.5 indicates that the avalanche ionization process is most likely involved, leading towards catastrophic damage. Analysis of the fatigue effect has shown that catastrophic damage is pulse duration dependent at both IR and UV wavelengths while color mode associated fatigue was almost insensitive to the pulse duration.

Funding. European Regional Development Fund under grant agreement with the Research Council of Lithuania (LMTLT) (01.2.2-LMT-K-718-03-0004).

Acknowledgements. The authors acknowledge UAB Optolita for a donation of experimental samples.

Disclosures. The authors declare no conflicts of interest.

Data availability. Data underlying the results presented in this paper are not publicly available at this time but may be obtained from the authors upon reasonable request.

References

1. S. Gales, K. Tanaka, D. Balabanski, F. Negoita, D. Stutman, O. Tesileanu, C. Ur, D. Ursescu, I. Andrei, S. Ataman, M. Cernaianu, L. D'Alessi, I. Dancus, B. Diaconescu, N. Djourelov, D. Filipescu, P. Ghenuche, D. G. Ghita, C. Matei, and N. Zamfir, "The extreme light infrastructure—nuclear physics (eli-np) facility: new horizons in physics with 10 pw ultra-intense lasers and 20 mev brilliant gamma beams," (2018).
2. N. Blanchot, G. Béhar, J. Chapuis, C. Chappuis, S. Chardavoine, J. Charrier, H. Coïc, C. Damiens-Dupont, J. Duthu, P. Garcia, J. P. Goossens, F. Granet, C. Grosset-Grange, P. Guerin, B. Hebrard, L. Hilsz, L. Lamaignere, T. Lacombe, E. Lavastre, T. Longhi, J. Luce, F. Macias, M. Mangeant, E. Mazataud, B. Minou, T. Morgaint, S. Noailles, J. Neauport, P. Patelli, E. Perrot-Minnot, C. Present, B. Remy, C. Rouyer, N. Santacreu, M. Sozet, D. Valla, and F. Laniesse, "1.15 pw-850 j compressed beam demonstration using the petal facility," Opt. Express **25**(15), 16957–16970 (2017).
3. B. C. Stuart, M. D. Feit, S. Herman, A. M. Rubenchik, B. W. Shore, and M. D. Perry, "Optical ablation by high-power short-pulse lasers," J. Opt. Soc. Am. B **13**(2), 459–468 (1996).
4. M. Lenzner, J. Krüger, S. Sartania, Z. Cheng, C. Spielmann, G. Mourou, W. Kautek, and F. Krausz, "Femtosecond optical breakdown in dielectrics," Phys. Rev. Lett. **80**(18), 4076–4079 (1998).
5. M. Mero, J. Liu, W. Rudolph, D. Ristau, and K. Starke, "Scaling laws of femtosecond laser pulse induced breakdown in oxide films," Phys. Rev. B **71**(11), 115109 (2005).
6. E. S. Bliss, "Pulse duration dependence of laser damage mechanisms," Opt. Quantum Electron. **3**(2), 99–108 (1971).
7. R. M. Wood, *Laser-Induced Damage of Optical Materials* (CRC Press, 2003), 1st ed.
8. O. M. Efimov, S. Juodkazis, and H. Misawa, "Single- and multiple-pulse laser-induced breakdown in transparent dielectrics in the femto-nanosecond region," in *Laser-Induced Damage in Optical Materials: 2003*, vol. 5273 G. J. Exarhos, A. H. Guenther, N. Kaiser, K. L. Lewis, M. J. Soileau, and C. J. Stolz, eds., International Society for Optics and Photonics (SPIE, 2004), pp. 61–73.
9. M. H. Niemz, "Threshold dependence of laser-induced optical breakdown on pulse duration," Appl. Phys. Lett. **66**(10), 1181–1183 (1995).
10. J. Krüger, M. Lenzner, S. Martin, M. Lenner, C. Spielmann, A. Fiedler, and W. Kautek, "Single- and multi-pulse femtosecond laser ablation of optical filter materials," Appl. Surf. Sci. **208-209**, 233–237 (2003).
11. L. Gallais, B. Mangote, M. Zerrad, M. Commandré, A. Melninkaitis, J. Mirauskas, M. Jeskevic, and V. Sirutkaitis, "Laser-induced damage of hafnia coatings as a function of pulse duration in the femtosecond to nanosecond range," Appl. Opt. **50**(9), C178–C187 (2011).
12. D. Du, X. Liu, G. Korn, J. Squier, and G. Mourou, "Laser-induced breakdown by impact ionization in sio2 with pulse widths from 7 ns to 150 fs," Appl. Phys. Lett. **64**(23), 3071–3073 (1994).
13. A. Rosenfeld, M. A. Lorenz, R. Stoian, and D. Ashkenasi, "Ultrashort-laser-pulse damage threshold of transparent materials and the role of incubation," Appl. Phys. A **69**(7), S373–S376 (1999).

Optics EXPRESS

14. J.-L. Déziel, L. J. Dubé, and C. Varin, "Dynamical rate equation model for femtosecond laser-induced breakdown in dielectrics," Phys. Rev. B **104**(4), 045201 (2021).
15. Y. Furukawa, S. A. Markgraf, M. Sato, H. Yoshida, T. Sasaki, H. Fujita, T. Yamanaka, and S. Nakai, "Investigation of the bulk laser damage of lithium triborate, lib3o5, single crystals," Appl. Phys. Lett. **65**(12), 1480–1482 (1994).
16. A. Melninkaitis, D. Mikšys, R. Grigonis, V. Sirutkaitis, M. Jupé, and D. Ristau, "Comparative studies of laser-induced damage threshold measurements in highly reflecting mirrors," in *Laser-Induced Damage in Optical Materials: 2007*, vol. 6720 G. J. Exarhos, A. H. Guenther, K. L. Lewis, D. Ristau, M. J. Soileau, and C. J. Stolz, eds., International Society for Optics and Photonics (SPIE, 2007), pp. 371–378.
17. A. V. Smith and B. T. Do, "Bulk and surface laser damage of silica by picosecond and nanosecond pulses at 1064 nm," Appl. Opt. **47**(26), 4812–4832 (2008).
18. F. Kong, Y. Jin, D. Li, W. Chen, M. Zhu, T. Wang, C. Li, H. He, G. Xu, and J. Shao, "Effect of pulse duration on laser induced damage threshold of multilayer dielectric gratings," in *Laser-Induced Damage in Optical Materials: 2012*, vol. 8530 G. J. Exarhos, V. E. Gruzdev, J. A. Menapace, D. Ristau, and M. J. Soileau, eds., International Society for Optics and Photonics (SPIE, 2012), pp. 125–133.
19. A. Das, A. Wang, O. Uteza, and D. Grojo, "Pulse-duration dependence of laser-induced modifications inside silicon," Opt. Express **28**(18), 26623–26635 (2020).
20. G. Duchateau and A. Dyan, "Coupling statistics and heat transfer to study laser-induced crystal damage by nanosecond pulses," Opt. Express **15**(8), 4557–4576 (2007).
21. G. Duchateau, "Simple models for laser-induced damage and conditioning of potassium dihydrogen phosphate crystals by nanosecond pulses," Opt. Express **17**(13), 10434–10456 (2009).
22. A. Dyan, F. Enguehard, S. Lallich, H. Piombini, and G. Duchateau, "Scaling laws in laser-induced potassium dihydrogen phosphate crystal damage by nanosecond pulses at 3ω," J. Opt. Soc. Am. B **25**(6), 1087–1095 (2008).
23. A. Chmel, "Fatigue laser-induced damage in transparent materials," Mater. Sci. Eng., B **49**(3), 175–190 (1997).
24. S. Möller, A. Andresen, C. Merschjann, B. Zimmermann, M. Prinz, and M. Imlau, "Insight to uv-induced formation of laser damage on lib3o5 optical surfaces during long-term sum-frequency generation," Opt. Express **15**(12), 7351–7356 (2007).
25. H. Hong, Q. Liu, L. Huang, and M. Gong, "Improvement and formation of uv-induced damage on lbo crystal surface during long-term high-power third-harmonic generation," Opt. Express **21**(6), 7285–7293 (2013).
26. K. M. Davis, K. Miura, N. Sugimoto, and K. Hirao, "Writing waveguides in glass with a femtosecond laser," Opt. Lett. **21**(21), 1729–1731 (1996).
27. L. Smalakys, E. Drobužaitė, B. Momgaudis, R. Grigutis, and A. Melninkaitis, "Quantitative investigation of laser-induced damage fatigue in hfo2 and zro2 single layer coatings," Opt. Express **28**(17), 25335–25345 (2020).
28. L. Smalakys, B. Momgaudis, R. Grigutis, S. Kičas, and A. Melninkaitis, "Contrasted fatigue behavior of laser-induced damage mechanisms in single layer zro2 optical coating," Opt. Express **27**(18), 26088–26101 (2019).
29. A. Ollé, J. Luce, N. Roquin, C. Rouyer, M. Sozet, L. Gallais, and L. Lamaignère, "Implications of laser beam metrology on laser damage temporal scaling law for dielectric materials in the picosecond regime," Rev. Sci. Instrum. **90**(7), 073001 (2019).
30. "Lasers and laser-related equipment — test methods for laser-induced damage threshold — part 2: Threshold determination," ISO 21254-2:2011(en).
31. L. V. Keldysh, "Ionization in the field of a strong electromagnetic wave," Zh. Eksperim. i Teor. Fiz. **45**, 1945–1957 (1964).
32. A. Kaiser, B. Rethfeld, M. Vicanek, and G. Simon, "Microscopic processes in dielectrics under irradiation by subpicosecond laser pulses," Phys. Rev. B **61**(17), 11437–11450 (2000).
33. B. Rethfeld, "Unified model for the free-electron avalanche in laser-irradiated dielectrics," Phys. Rev. Lett. **92**(18), 187401 (2004).
34. B. Momgaudis, V. Kudriasov, M. Vengris, and A. Melninkaitis, "Quantitative assessment of nonlinearly absorbed energy in fused silica via time-resolved digital holography," Opt. Express **27**(5), 7699–7711 (2019).
35. A.-C. Tien, S. Backus, H. Kapteyn, M. Murnane, and G. Mourou, "Short-pulse laser damage in transparent materials as a function of pulse duration," Phys. Rev. Lett. **82**(19), 3883–3886 (1999).